1 Bidirectional supramolecular display and signal

2 amplification on the surface of living cells

- 3 Brandon Davis, Peng Shi, Erin Gaddes, Jinping Lai, and Yong Wang*
- 4 Department of Biomedical Engineering, The Pennsylvania State University, University Park,
- 5 Pennsylvania 16802, USA
- 6 KEYWORDS: Cell surface engineering, DNA self-assembly, reversible polymerization,
- 7 fluorescent amplification.

8

14

holds great potential for biomedical applications such as cell imaging and delivery. Numerous methods have been well-established to enhance the display of biomolecules and nanomaterials on the cell surface. However, it is challenging to remove these biomolecules or nanomaterials from the cell surface. The purpose of this study was to investigate the reversible display of supramolecular nanomaterials on the surface of living cells. The data show that DNA initiators

ABSTRACT. The ability to display exogenous molecules or nanomaterials on the surface of cells

and amplify the fluorescence signals on the cell surface. Complementary DNA (cDNA), DNase,

could induce the self-assembly of DNA-alginate conjugates to form supramolecular nanomaterials

- and alginase could all trigger the reversal of the signals from the cell surface. However, these three
- molecules exhibited different triggering efficiency with the order of cDNA>alginase>DNase. The
- 18 combination of cDNA and alginase led to synergistic reversal of nanomaterials and fluorescent

- 19 signals from the cell surface. Thus, this study has successfully demonstrated a method for
- bidirectional display of supramolecular nanomaterials on the surface of living cells. This method
- 21 may find its application in numerous fields such as intact cell imaging and separation.

1. INTRODUCTION

22

23

24

25

26

27

28

29

30

31

32

33

34

35

36

37

38

39

40

41

42

43

44

Great effort has been made to develop methods for displaying exogenous molecules and nanomaterials on the surface of living cells in applications such as tissue engineering, cell delivery, cell imaging, and cell separation. 1-8 It is equally important to remove these molecules or nanomaterials from the cell surface in numerous applications. 9-11 For instance, the surface display of fluorescent molecules or nanomaterials has been widely used for cell imaging and separation. 12-¹⁴ However, if the imaged cells need re-imaging or the separated cells need further evaluation or in vivo delivery, these molecules or nanomaterials may cause problems. 15,16 Therefore, the ability to reversibly display molecules or nanomaterials on the cell surface can offer benefits for certain applications which traditional methods do not offer. The reversible display has two essential requirements. One is to strengthen the display; the other is to dissociate or degrade the displayed molecules or materials. The strong display can be achieved by covalently conjugating molecules or nanomaterials on the cell surface. 5,17,18 However, it is difficult to break covalent bonds for the reversible removal of the conjugated molecules or nanomaterials. 19,20 The display can also be achieved using physical interactions. 21–24 For example, molecules or nanomaterials conjugated with hydrophobic moieties (e.g., cholesterol) can be displayed on the cell surface through molecular insertion into the lipid bilayer. ^{25–28} While physical interactions are weaker than covalent conjugation, it remains difficult to actively reverse the display of molecules and nanomaterials from the cell surface. 2,29,30 In principle, physical interactions can be reversed using numerous methods such as high temperature, acidic treatment and protease degradation. ^{31–34} These methods can be applied to treat fixed cells. For instance, the Gao Group developed an elegant method for displaying quantum dots on the surface of fixed cells. ^{35–37} The quantum dots can be reversed from the cell surface by treating

the cells with a regeneration buffer with pH 2.8 and 0.5% SDS. However, while this method works successfully for the reversible display of nanomaterials, it will be detrimental to living cells or cell surface components. Thus, it remains challenging to actively reverse exogenous molecules and nanomaterials from the surface of living cells under mild conditions.

The purpose of this work was to explore a method for bidirectional supramolecular display using hybrid DNA-alginate conjugates and triggering molecules. The first step of this method is the display of a supramolecular DNA-alginate nanomaterial. This nanomaterial has multiple repeating units. Each unit contains an alginate molecule conjugated with multiple molecules (e.g., fluorophores and biotin). We studied the display of the supramolecular DNA-alginate nanomaterial on the cell surface using lipid insertion. The second step of this method is cell treatment with triggering molecules for the reversible display. We studied three types of triggering molecules including complementary DNA (cDNA) sequences, DNase, and alginase. The combination of these triggering molecules was also examined to study the synergy of triggering molecules in reversing the supramolecular nanomaterial from the cell surface.

2. EXPERIMENTAL

2.1. Materials

45

46

47

48

49

50

51

52

53

54

55

56

57

58

- DNA oligonucleotide sequences (Table S1) were purchased from Integrated DNA Technologies
- 62 (Coralville, IA). Dibenzocyclooctyne (DBCO) reagents, including DBCO-PEG₄-NHS ester,
- DBCO-Cy5 and DBCO-PEG₄-Biotin were purchased from Click Chemistry Tools (Scottsdale,
- 64 AZ). Medium viscosity Sodium alginate (A2033, molecular weight: 80,000-120,000 Da), O-(2-
- 65 Aminoethyl)-O'-(2-azidoethyl)pentaethylene glycol (NH₂-PEG₆-N₃), 2-(N-
- Morpholino)ethanesulfonic acid sodium salt (MES sodium salt), N-hydroxysuccinimide (NHS),
- 67 1-ethyl-3-(3-dimethylaminopropyl)carbodiimide hydrochloride (EDC), sodium hydroxide

- 68 (NaOH), anhydrous dimethyl sulfoxide (DMSO), alginate lyase (alginase), and Dulbecco's
- 69 Modified Eagle's Medium (DMEM) were purchased from Sigma-Aldrich (St. Louis, MO).
- Acetone, sodium bicarbonate (NaHCO₃), and DNase I were purchased from Fisher Scientific
- 71 (Pittsburgh, PA). Dulbecco's phosphate buffered saline (DPBS), fetal bovine serum
- 72 (FBS), and Roswell Park Memorial Institute (RPMI)-1640 medium were purchased from Gibco
- 73 (Gaithersburg, MD). Streptavidin PE-Cy5.5 probes were purchased from Invitrogen (Carlsbad,
- 74 CA).

75

2.2. Preparation of Azide-modified Alginate (Alginate-N₃)

- Azide-modified alginate (alginate-N₃) was prepared through NHS/EDC coupling of carboxyl
- groups. ³⁸ First, 100 mg of sodium alginate was dissolved in 10 mL of MES buffer (50 nM, pH=5).
- Next, 28 mg NHS, 232 mg EDC, and 56 µL NH₂-PEG₆-N₃ were added to the sodium alginate
- 79 solution and stirred for 30 minutes. The pH was adjusted to 7.5 with 6 M NaOH and the reaction
- 80 proceeded overnight at room temperature. Alginate-N₃ was purified of unreacted reagents by
- 81 dialysis (10 kDa molecular weight cut-off) against ddH₂O, followed by precipitation in chilled
- 82 acetone.

2.3. Preparation of DBCO-modified DNA Monomer 2 (DM2-DBCO)

- DM2-DBCO conjugates were formed through amine-reactive crosslinker chemistry. ^{38,39} After
- 85 preparing a 30 mM solution of DBCO-PEG₄-NHS ester, 100 μL DM2-NH₂ was mixed with 25 μL
- of DBCO-PEG₄-NHS ester in a NaHCO₃ buffer (50 nM) and allowed to react for 6 hours at room
- 87 temperature. This reaction was repeated a total of 3 times. Excess DBCO-PEG₄-NHS ester linkers
- were removed by centrifugal filtration (3 kDa MWCO). The concentration of purified DM2-
- 89 DBCO was determined by spectrophotometric analysis of the nucleic acid (λ =260 nm) on a
- 90 ThermoScientific Nanodrop 2000 spectrophotometer (Waltham, MA).

2.4. Preparation of DM2-Alginate Conjugates

Alginate-N₃ and DM2-DBCO were covalently crosslinked via a copper-free click chemistry reaction.³⁸ DM2-DBCO was mixed with alginate-N₃ (1% w/v) at a 3:1 molar ratio and reacted for 2 hours. DM2-alginate was collected and purified of excess DM2-DBCO by centrifugal filtration (100 kDa MWCO). DM2-alginate was further modified with either biotin or fluorescent molecules. Either DBCO-PEG₄-Biotin or DBCO-Cy5 was mixed with DM2-alginate conjugates at a 3:1 ratio and reacted for 2 hours. Sample was collected and purified by centrifugal filtration (100 kDa MWCO). Polyacrylamide gel electrophoresis was used to assess the DM2-alginate conjugation reaction.

2.5. Evaluation of Bidirectional DNA Polymerization via Gel Electrophoresis

Prior to polymerization, FAM-labeled DNA monomer 1 (DM1-FAM) and Cy5-labeled DM2-alginate (DM2-alginate-Cy5) were heated to 95 °C for 5 minutes using a Bio-Rad T11 Thermal Cycler (Hercules, CA) and cooled at room temperature for 1 hour to ensure hairpin conformation. For hybridization, DNA monomer sequences were mixed at a 10:1 molar ratio with DI for 2 hours at room temperature in DPBS buffer. To degenerate DNA polymers, various triggering molecules were incubated with DNA polymers for 1 hour at room temperature in DPBS buffer. For T_{DNA}, complementary sequences to DM1-FAM and DI were added at a 2:1 molar ratio. For DNase, 1 unit of DNase was added to DNA polymers. For alginase, 0.01 units of alginase was added to DNA polymers. Samples were loaded into the wells of a 10% (w/v) polyacrylamide gel and run for 40 min at 80 V in 1×TBE buffer. Gels were subsequently imaged using a CRI Maestro In-Vivo imaging system (Woburn, MA) to observe the fluorescently labeled DNA. Maestro 3.0.1 software was used to process gel images.

2.6. Cell Culture

Cell labeling experiments were performed using human acute lymphoblastic leukemia (CCRF-CEM) and mouse endothelial (C166) cell lines purchased from ATCC (Manassas, VA). Human acute lymphoblastic leukemia cells (CCRF-CEM) were maintained in RPMI-1640 medium supplemented with 10% fetal bovine serum (FBS). Mouse endothelial cells (C166) were maintained in DMEM medium supplemented with 10% FBS. Cells were incubated at 37°C with an atmosphere of 5% CO₂ and 95% relative humidity.

2.7. Supramolecular Assembly on the Cell Surface

Supramolecular assembly (SMA) on the cell surface was studied using both suspension and adherent cells, i.e., CCRF-CEM and C166 cells.

CCRF-CEM cells were rinsed with DPBS and resuspended at 1×10^6 cells/mL. Cholesterol-modified DNA initiators (DI-Cholesterol) were added to CCRF-CEM cells to a final concentration of 50 nM. Excess DI-Cholesterol molecules were removed from DI-modified CCRF-CEM cells (DI-cells) with DPBS rinsing thrice. DI-cells were treated with DNA monomers according to conditions shown in Table S2 to generate supramolecular DNA nanomaterials. To generate Alginate labeled samples, cells were treated sequentially with DM1-FAM and DM2-alginate-biotin at room temperature for 1.5 hours. All other samples were incubated with DNA for 3 hours at room temperature. Samples were then rinsed three times with DPBS to remove excess oligonucleotides. Supramolecular DNA nanomaterials were labeled with fluorescent streptavidin probes. 2 μ L Streptavidin-PE-Cy5.5 (0.05 mg/mL) were added to resuspended samples for 30 minutes at room temperature before flow cytometry and fluorescence imaging. Supramolecular assembly was also studied on the surface of C166 cells using an identical process.

2.8. Removal of Nanomaterials from the Cell Surface

The supramolecular nanomaterials were reversed following the addition of triggering molecules including complementary DNA trigger sequences (T_{DI}, T_{DM1}), DNase and alginate lyase. Cell samples were treated with the triggering molecules using the conditions as shown in Table S3. All triggering reactions were conducted for 30 minutes at room temperature. Samples were rinsed three times with DPBS to remove triggering molecules prior to analysis by flow cytometry or fluorescence imaging.

2.9. Cell Imaging and Analysis

Cells were examined using flow cytometry and fluorescence imaging. Mean fluorescent intensity was measured by flow cytometry analysis on an EMD Millipore Guava easyCyte flow cytometer (Hayward, CA) for all samples. Signal-to-noise ratio (SNR) was calculated for the fluorescent amplification samples using Equation 1.⁴⁰

$$SNR = \frac{\mu_{sample}}{\sigma_{unlabeled}}$$
 Eq. 1

The remaining fluorescent signal of triggered SMA samples was calculated as a percentage of the initial SMA intensity using Equation 2.

Intensity (%) =
$$\frac{\mu_{\text{sample}}}{\mu_{\text{SMA}}} * 100$$
 Eq. 2

Fluorescent images were captured on an Olympus IX73 inverted microscope (Center Valley, PA) for each labeled and triggered sample using a consistent exposure time and lamp intensity. ImageJ software was used to derive line profile data from representative images. Localized intensity data was collected from a single line drawn across a single cell in each representative image as shown in the inset image.

2.10. Statistical Analysis

159

160

161

162

163

164

165

166

167

168

169

170

171

172

173

174

175

176

177

178

179

180

Statistical significance between mean values was determine using Prism GraphPad V9.2.0 statistical software. A Brown-Forsythe's ANOVA and multiple unpaired Welch's t tests were used to determine P-value between sample means. A P-value of ≤0.05 was used to indicate statistical significance.

3. RESULTS AND DISCUSSION

3.1. Assembly and Disassembly of Supramolecular DNA-Alginate Nanomaterials

Supramolecular DNA-based nanomaterials were synthesized on the cell surface through the assembly of DNA-polymer conjugates. The polymer used in this work was alginate. We chose alginate for two reasons. First, alginate is a natural polysaccharide with many hydroxyl or carboxyl groups that can be modified with interesting molecules such as oligonucleotides, fluorophores and biotin.⁴¹ Second, alginate is different from any component on the cell surface. Alginate can be degraded by alginase; however, the use of alginase will not cause the degradation of natural cell surface components. To synthesize DNA-alginate conjugates, alginate was first modified with azide groups via EDC/NHS coupling and subsequently conjugated with DBCO-modified DM2 by copper-free click chemistry (Figure 1A). DM2-alginate conjugates were analyzed using spectrophotometer for the presence of DM2 molecules after purification of the conjugation solution (Figure 1B). The conjugation solution exhibited the same peak absorbance at 260 nm as the free DM2 solution. This result shows that DM2 was successfully conjugated to alginate. We further ran gel electrophoresis to analyze the conjugation of DM2 to alginate. In contrast to unconjugated DM2 and Cy5-labeled alginate without DNA, DM2-alginate-Cy5 conjugates displayed a localization of both alginateCy5 and DM2 signals. Thus, the gel electrophoresis result is consistent with the spectrophotometric analysis (Figure 1C), confirming the formation of DM2-alginate conjugates. The conjugation of a large polymer to DNA may interfere with the hybridization potential of the DNA strands. Thus, we assessed whether DM2-alginate-Cy5 conjugates could hybridize with DM1-FAM and participate in the hybridization chain reaction (HCR) (Figure 1D).⁴² A gel electrophoresis experiment was conducted to examine the hybridization potential of DM2-alginate conjugates. The subsequent de-polymerization of the hybridized DNA polymer in the presence of different triggering molecules was also examined (Figure 1E). In contrast to the separation of DM1-FAM and DM2-alginate-Cy5 in Lane 3, the localization of FAM-labeled DM1 sequences and DM2-alginate-Cy5 conjugates in Lane 4 confirmed the conjugates retain their hybridization capacity in the presence of the DI sequence (Figure 1F). The triggered separation of DM1-FAM and DM2-alginate-Cy5 in Lanes 5-7 indicated that the triggering molecules can deconstruct the components of the DNA-polymer nanomaterials (Figure 1F). Specifically, the upward shift of the DNA band in Lane 5 supports the hybridization of a complementary sequence to DM1-FAM. Inversely, the downward shift in Lane 6 validates the degradation of DNA into significantly shorter sequences by DNase. Interestingly, the removal of the Cy5 signal in Lane 7 indicates alginate can be degraded without altering the DNA sequences. This is reasonable as alginate is a side chain of the supramolecular DNA backbone. Taken together, these results suggest that DNA-polymer conjugates can participate in the formation of supramolecular nanomaterials and the nanomaterials can be disassembled or degraded in the presence of triggering molecules.

181

182

183

184

185

186

187

188

189

190

191

192

193

194

195

196

197

198

199

200

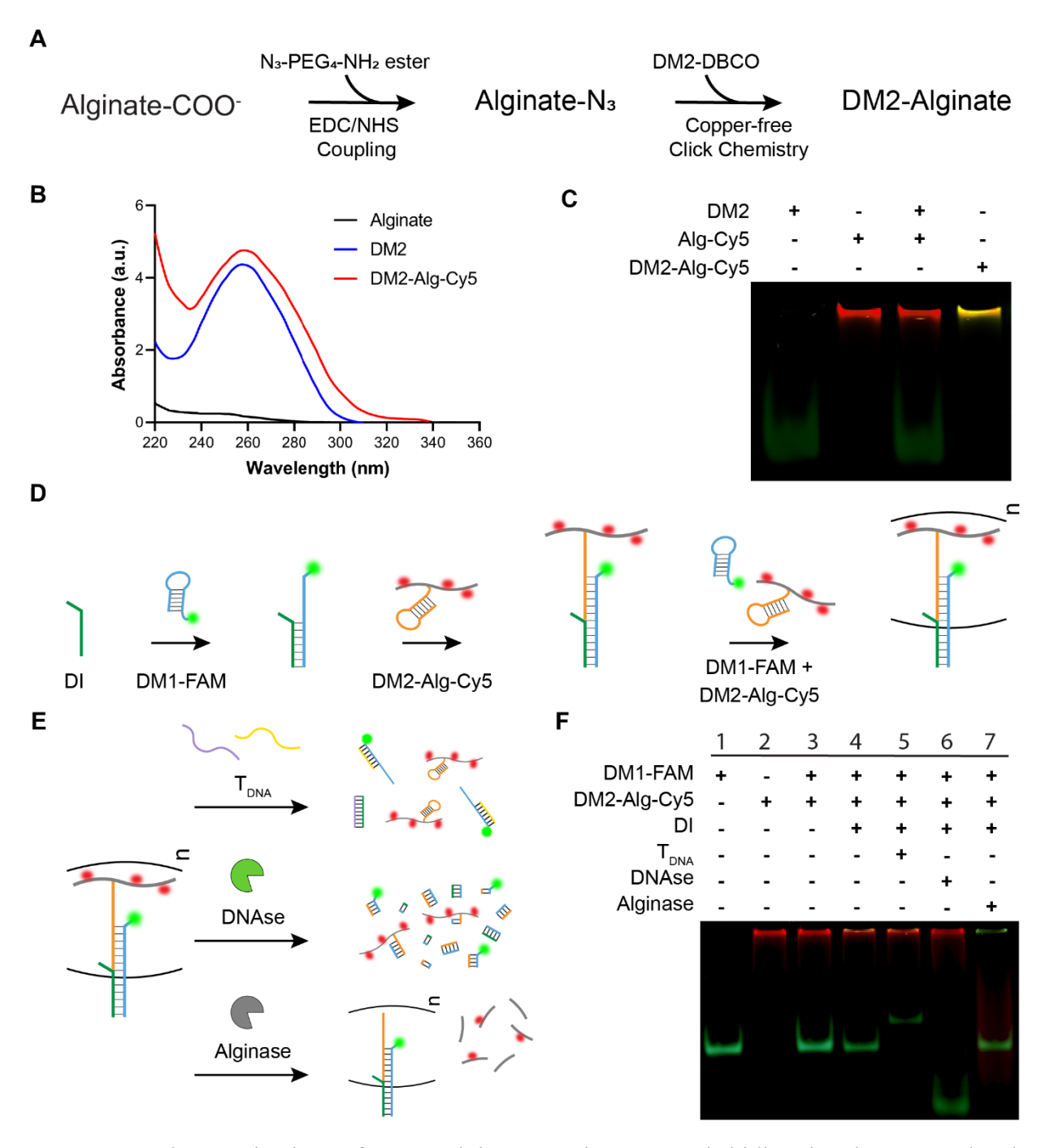


Figure 1: Characterization of DNA-alginate conjugates and bidirectional supramolecular assembly. (A) Synthesis of DM2-alginate conjugate via EDC/NHS coupling and copper-free click chemistry. (B) Absorption spectra of alginate, DM2 and DM2-alginate conjugate. (C) Gel image depicting conjugation of DM2-alginate-Cy5 conjugate. SYBRSafe was used to stain double-stranded DNA. (D) Scheme of supramolecular assembly. (E) Scheme of supramolecular disassembly or degradation. (F) Gel image depicting assembly and disassembly or degradation. DI: DNA initiator; Alg: alginate; DM2-Alg-Cy5: Alginate conjugated with DM2 and Cy5; T_{DNA}: triggering cDNAs of DI & DM1.

3.2. Supramolecular Assembly and Signal Amplification on the Cell Surface

211

212

213

214

215

216

217

218

219

220

221

222

223

224

225

226

227

228

229

To achieve supramolecular assembly on the cell surface, the cell membrane was first decorated with cholesterol-conjugated DI based on lipid insertion (Figure 2A). Multiple controls were designed to illustrate DI-initiated supramolecular assembly and signal amplification on the cell surface (Figure 2B). Specifically, the FAM group and the Alginate group each display a single DM1 which has been labeled with FAM (Figure 2B). Unlike the FAM group, the Alginate group contains a single hybridization unit with one DM1-FAM and one DM2-alginate-biotin conjugate that can bind more than one streptavidin. The PE-Cy5.5 group has one streptavidin that was used to label a biotinylated cDNA to DI. With these controls, we could evaluate the assembly and signal amplification in the Supramolecular Assembly (SMA) group through the examination of the two fluorophores. The flow cytometry analysis showed that the cells in the SMA group exhibited a FAM intensity five times higher than in the FAM and Alginate groups (Figures 2C and 2D). This difference clearly demonstrates that the supramolecular assembly of DM1 and DM2-alginate conjugates led to the formation of a DNA-based nanomaterial consisting of multiple repeating units. We further used fluorescence microscopy to examine the FAM intensity of the cell surface. Representative line profiles were drawn across the cells. The cell imaging analysis (Figure 2E) showed that the cells in the SMA group exhibited the highest FAM intensity, further confirming the results of the flow cytometry.

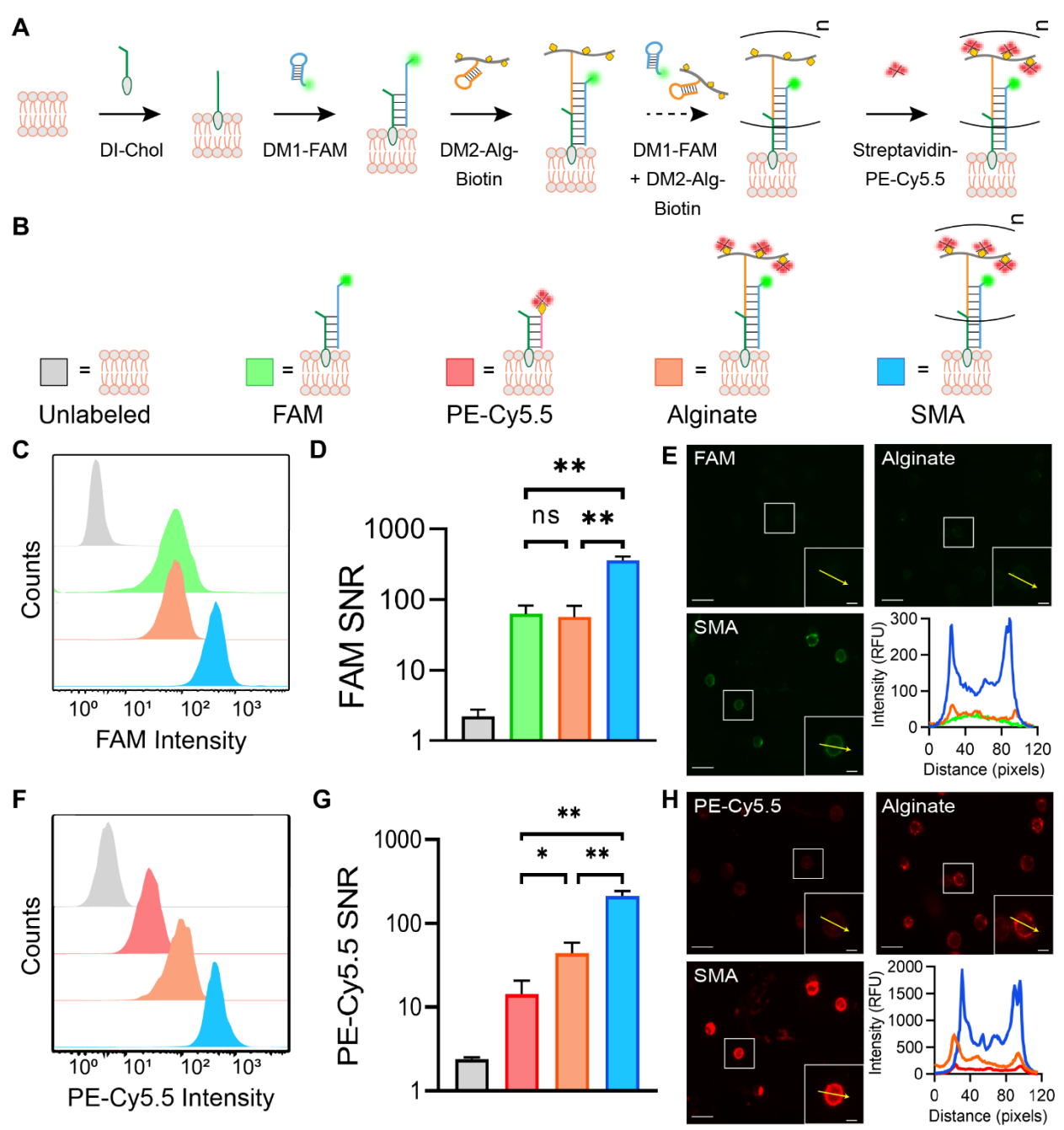


Figure 2: Examination of supramolecular assembly and signal amplification on the cell surface. (A) Schematic illustration of supramolecular assembly on the cell surface. (B) Schematic representation of experimental groups. SMA: supramolecular assembly. (C-E) Comparison of signal intensity of FAM in different groups. (F-H) Comparison of signal intensity of PE-Cy5.5 in different groups. Streptavidin-PE-Cy5.5 bound biotin-CS_{DI} conjugates or biotin-DM2-alginate conjugates. (C and F) Flow cytometry analysis. (D and G) Signal-to-noise ratio (SNR). (E and H) Fluorescence live cell images and corresponding line intensity profiles for arrows depicted in image inset. Scale bars: 20 μm (inset scale bars: 5 μm). RFU: relative fluorescent units. ns: not significant, *: p<0.05, **: p<0.01.

As the DM2-alginate conjugate was further conjugated with biotin, the nanomaterial could bind to streptavidin-PE-Cy5.5 through streptavidin-biotin interactions. The cells in the Alginate group exhibited PE-Cy5.5 intensity nearly three times higher than the PE-Cy5.5 group (**Figures 2F and 2G**). As the Alginate-labeled sample contains only a single DM2-alginate conjugate, this result demonstrates the ability of using biotinylated alginate to amplify the display of a fluorophore on the cell surface. The PE-Cy5.5 signal intensity was further increased by nearly five times in the SMA group (**Figures 2F and 2G**). Totally, the PE-Cy5.5 signal intensity was increased by ~15 times due to the use of biotinylated alginate and the HCR. The imaging analysis (**Figure 2H**) was consistent with the flow cytometry assessment. Thus, the data suggest that supramolecular assembly and signal amplification can be achieved on the surface of living cells.

3.3. cDNA-mediated Removal of Nanomaterials from the Cell Surface

Signal amplification can be achieved using different methods. For instance, instead of using the in-situ formation of supramolecular nanomaterials as shown in this work, nanomaterials can be first prepared and then applied to modify the cell surface. 43–46 However, the challenge is how to remove those nanomaterials from the cell surface after their display and signal amplification. The reversible display of nanomaterials and biomolecules on the cells surface is critical for downstream applications. 47 For example, the removal of fluorophore labels after detection grants the ability to utilize samples for multiplex imaging without the need for complex signal processing. 48 Another example is in vivo cell delivery after cell imaging and separation. 49 With less foreign materials left on the cell surface, there is a better chance to maintain cellular functions and avoid undesired immune response. 50–52 Thus, after showing the supramolecular display and signal amplification, we studied the removal of the supramolecular nanomaterials from the cell surface.

In our method, the nanomaterial is made of DNA and alginate. These molecules can in principle be actively removed from the cell surface using strand displacement or enzymatic degradation.^{53–} ⁵⁷ We first used cDNA to trigger the dissolution of the nanomaterials and the reduction of the associated fluorescent signal based on the principle of strand displacement (Figure 3A). The two triggering cDNA molecules include complementary sequences to DI (T_{DI}) and DM1 (T_{DM1}). When the cells were treated with either T_{DI} or T_{DM1}, the FAM intensity on the cell surface was significantly decreased (Figure 3B). In addition, cell treatment with the combination of T_{DI} and T_{DM1} (i.e., T_{DNA}) led to over 95% decrease of the FAM intensity (**Figure 3C**). These data suggest that cDNA can trigger the dissociation of the DNA nanomaterial and the reversal of FAM signal. PE-Cy5.5 intensity also decreased simultaneously with the decrease of FAM intensity, confirming that cDNA can trigger the reversal of the nanomaterials. However, the degree of the reduction was much less for PE-Cy5.5 compared to FAM. The decrease of PE-Cy5.5 intensity in the presence of T_{DI}, T_{DM1} and T_{DNA} was 30, 38, and 57%, respectively (Figures 3E and 3F). Fluorescent cell imaging analysis (Figures 3D and 3G) is consistent with the flow cytometry analyses. As PE-Cy5.5 is the signal from streptavidin and streptavidin binds biotinylated alginate, we hypothesized that a portion of biotinylated alginate molecules may bind to cell surface components. To test the hypothesis and to enhance the removal of PE-Cy5.5, we further studied the application of enzymes for removing the nanomaterials. 3.4. Synergistic Removal of Nanomaterials from the Cell Surface Using cDNA and Alginase Two enzymes were studied, including DNase and alginase. DNase was assessed for its ability to degrade the DNA backbone of the supramolecular nanomaterial, while alginase was examined for

its ability to degrade alginate molecules. We also studied the effectiveness of the mixture of cDNA

262

263

264

265

266

267

268

269

270

271

272

273

274

275

276

277

278

279

280

281

282

and alginase in removing the supramolecular nanomaterial using the mixture of DNase and alginase for comparison (Figure 4A).

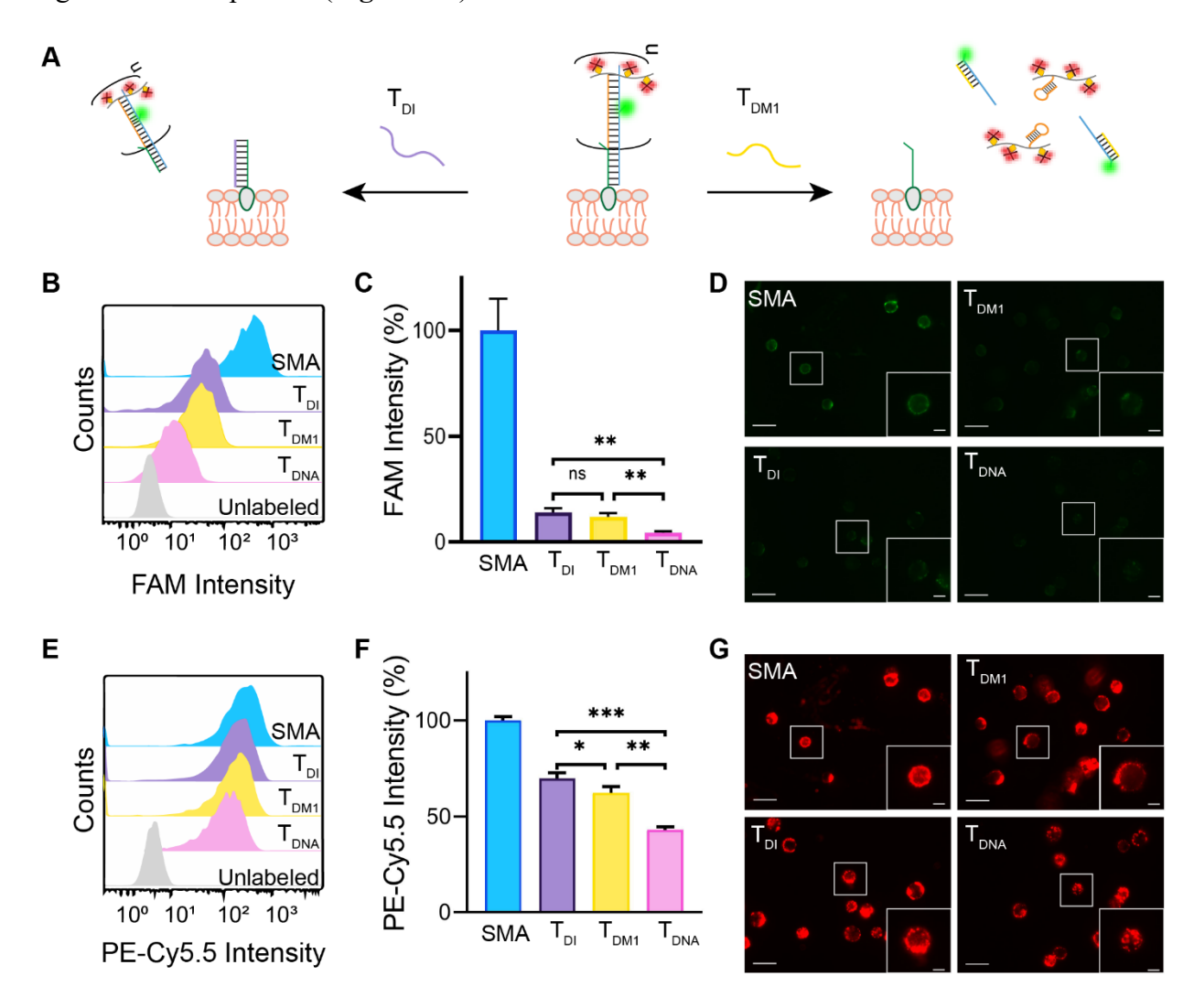


Figure 3: Evaluation of the function of triggering cDNA in disassembling the nanomaterial on the cell surface. (A) Schematic illustration of cDNA-based triggering. (B, C) Flow cytometry analysis of FAM signal. (D) Fluorescence live cell images of FAM signal. (E, F) Flow cytometry analysis of PE-Cy5.5 signal. (G) Fluorescence live cell images of PE-Cy5.5 signal. Scale bars: 20 μ m (inset scale bars: 5 μ m). SMA: supramolecular assembly; T_{DI} : triggering cDNA of DI; T_{DM1} : triggering cDNA of DM1; T_{DNA} : the combination of T_{DI} and T_{DM1} . Ns: not significant, *: p<0.05, **: p<0.01, ***: p<0.001.

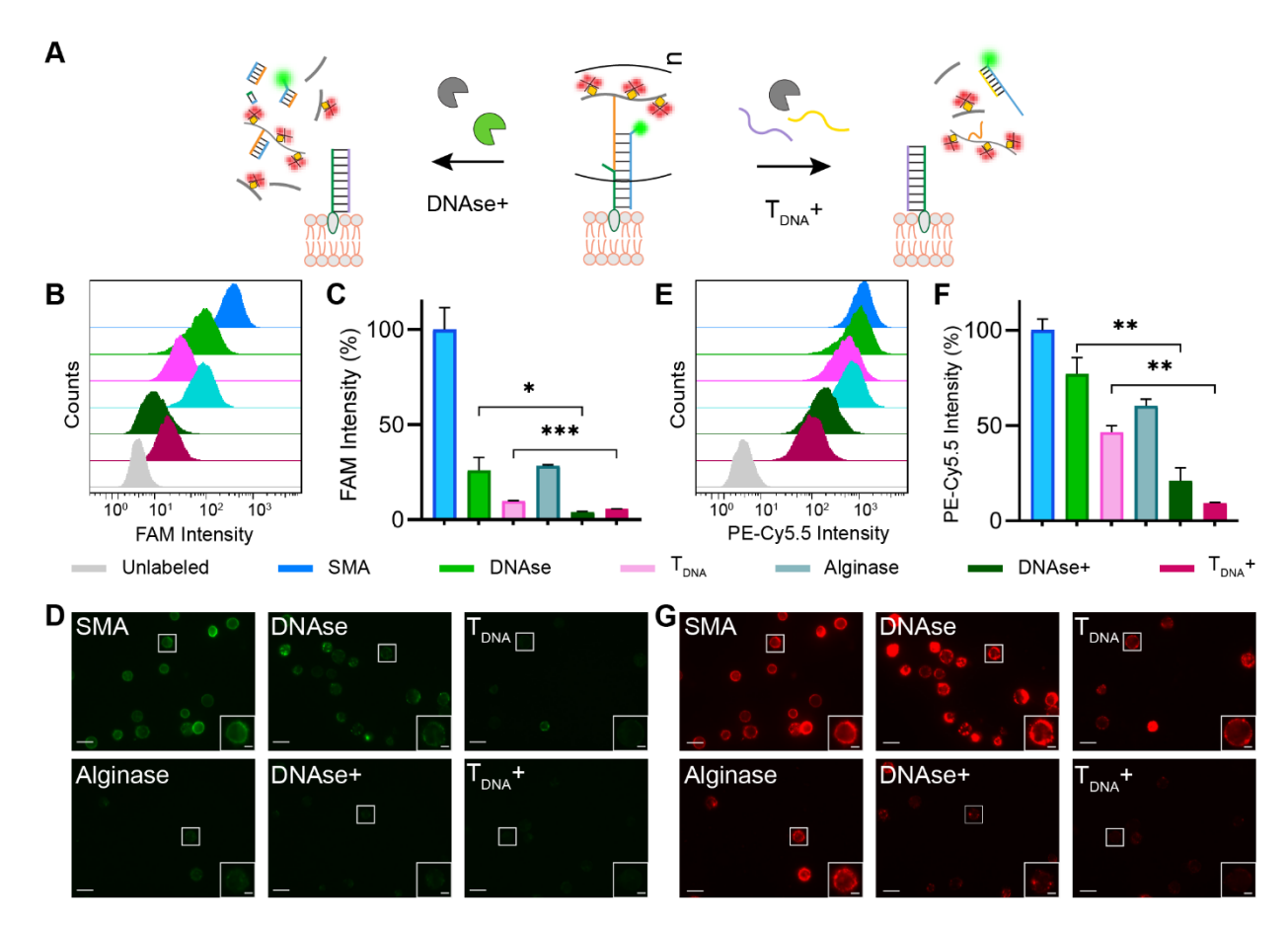


Figure 4: Evaluation of triggering synergy in disassembling the nanomaterial on the cell surface. (A) Schematic illustration of supramolecular nanomaterial removal. (B, C) Flow cytometry analyses of FAM signal. (D) Fluorescence live cell imaging for examination of FAM signal. (E, F) Flow cytometry analyses of PE-Cy5.5 signal. (G) Fluorescence live cell imaging for examination of PE-Cy5.5 signal. Scale bars: 20 μ m (inset scale bars: 5 μ m). SMA: supramolecular assembly; $T_{DNA}+:$ combination of T_{DNA} and alginase, DNase+: combination of DNase and alginase. *: p<0.05, **: p<0.01, ***: p<0.001.

DNase treatment was effective in reducing the FAM signal to 26% (**Figures 4B and 4C**). It suggests that DNase can degrade the DNA backbone of the nanomaterials. However, compared to cDNA treatment, DNase treatment had a much less significant impact on the PE-Cy5.5 signal with over 75% remaining on the cell surface (**Figures 4E and 4F**). These results, in combination with data shown in Figures 3F and 3G, suggest that alginate might remain on the cell surface. Thus, we further studied the effect of alginase treatment on the signal intensity of FAM and PE-Cy5.5. Alginase treatment decreased FAM signal intensity to 28% (**Figures 4B and 4C**), while 60% of

portion of alginate segments might still be linked with the DNA backbone. The data show that the capability of removing alginate and PE-Cy5.5 from the cell surface is T_{DNA}>alginase>DNase under experimental settings used in this study. Two mixtures were also prepared as triggering solutions for the removal of the nanomaterials and fluorophores from the cell surface. One mixture is the solution of DNase and alginase (i.e., DNase+); the other is the solution of T_{DNA} and alginase (i.e., T_{DNA}+). We could not prepare a mixture with both T_{DNA} and DNase as DNase can digest the triggering T_{DNA}. With the addition of alginase, DNase+ treatment decreased the signal intensity of FAM from 26% to 4% and T_{DNA}+ treatment decreased the signal intensity of FAM from 10% to 6% (Figures 4B and 4C). These data suggest that the mixture of two triggering molecules can lead to synergistic removal of DNA, DNA-alginate conjugates, and FAM from the cell surface. Alginase significantly improved the capabilities of both DNase and T_{DNA} in removing the PE-Cy5.5 signal (Figures 4E and 4F). Specifically, DNase+ reduced the PE-Cy5.5 signal intensity from 77% with DNase treatment alone to 21%. T_{DNA}+ treatment reduced the PE-Cy5.5 signal intensity from 47% with T_{DNA} treatment alone to 9% (Figures 4E and 4F). The fluorescence live cell imaging examination is consistent with these flow cytometry analyses (Figures 4D and 4G). As both enzymatic degradation and strand displacement are time-dependent interactions, we also examined the kinetics of nanomaterial disassembly. Under the same triggering conditions, the results suggest the nanomaterial disassembly and removal from the cell surface occurs primarily within the first 30 minutes of the trigger incubation (Figure S1). These results also show that alginase and cDNA can synergistically remove the DNA nanomaterial and fluorophore signals from the cell surface. However, it is also important to note that the signals could not be completely removed from the

the PE-Cy5.5 signal intensity remained on the cell surface (Figures 4E and 4F). It suggests that a

309

310

311

312

313

314

315

316

317

318

319

320

321

322

323

324

325

326

327

328

329

330

cell surface. It suggests that the residues of polymers were attached to the cell surface or might have already been internalized into the cells.

After showing that we could reversibly remove the DNA nanomaterials from the surface of non-adherent CCRF-CEM cells, we further explored this method using an adherent cell line (C166) to demonstrate the universal potential of bidirectional supramolecular display and signal amplification. Both DNase+ and T_{DNA}+ could reduce the fluorophore signal intensity (**Figures 5A and 5B**). However, T_{DNA}+ exhibited much higher efficiency of removing the signals of both FAM and PE-Cy5.5 from the cell surface than DNase+ (**Figures 5A and 5B**). The fluorescence live cell imaging examination is consistent with the flow cytometry analyses (**Figures 5C and 5D**). Taken together, the data suggest that the combination of T_{DNA} and alginase may be effective for bidirectional supramolecular display and signal amplification on a broad range of cells, including both adherent and non-adherent cells.

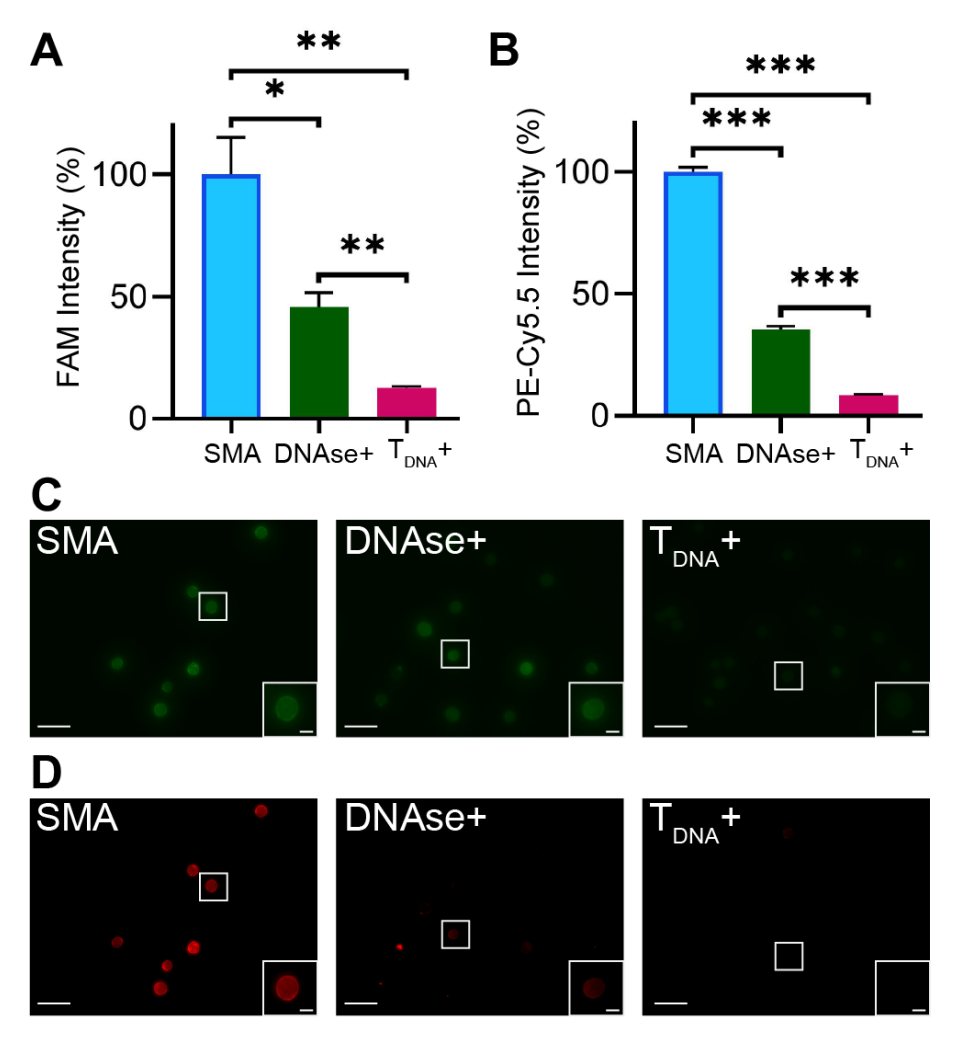


Figure 5: Evaluation of bidirectional supramolecular assembly and signal amplification on C166 cells. (A) Flow cytometry analysis of FAM signal. (B) Flow cytometry analysis of PE-Cy5.5 signal. (C) Fluorescence live cell images of FAM signal. (D) Fluorescence live cell images of PE-Cy5.5 signal. Scale bars: 20 μ m (inset scale bars: 5 μ m). SMA: supramolecular assembly; $T_{DNA}+:$ combination of T_{DNA} and alginase, DNase+: combination of DNase and alginase. *: p<0.05, **: p<0.01, ***: p<0.001.

4. CONCLUSION

This work has successfully shown supramolecular assembly of DNA-alginate conjugates on the cell surface. The assembly can lead to signal amplification. More importantly, the assembled nanomaterials can be removed from the surface of living cells in the presence of three different triggering molecules including cDNA, alginase, and DNase. These three triggering molecules have different efficiency in reversing the assembly with the order of cDNA>alginase>DNase. Cell

treatment with the combination of cDNA and alginase leads to synergistic nanomaterial removal and signal reversal on the cell surface. As the display of exogenous molecules or nanomaterials on the surface of living cells is important to many fields, we envision that this method for bidirectional display of supramolecular DNA-based nanomaterials on the surface of living cells will find numerous potential applications such as non-destructive cell separation, intact cell delivery and multiplex cell imaging.

ASSOCIATED CONTENT

357

358

359

360

361

362

363

364

369

375

Supporting Information.

- Figure S1 shows the kinetics of molecular disassembly and degradation . DNA sequences are
- listed in the Table S1. The concentrations of DNA nanomaterial components are listed in Table
- 367 S2. The composition of triggering reagents is listed in Table S3.

368 AUTHOR INFORMATION

Corresponding Author

- 370 *Yong Wang Department of Biomedical Engineering, The Pennsylvania State University,
- University Park, Pennsylvania 16802, USA. Email address: yxw30@psu.edu

372 **Author Contributions**

- 373 The manuscript was written through contributions of all authors. All authors have given approval
- 374 to the final version of the manuscript.

Funding Sources

376 This work is in part supported by the U.S. National Science Foundation (1802953 and 1911764).

- 377 Notes
- 378 The authors have filed a patent application based on the method presented in this work.
- 379 ACKNOWLEDGEMENTS
- The authors would like to thank the U.S. National Science Foundation (1802953 and 1911764 for
- 381 financial support. The authors would also like to thank James Coyne, Lidya Abune and Xuelin
- Wang for reading this manuscript.
- 383 REFERENCES
- 384 (1) Teramura, Y.; Iwata, H. Cell Surface Modification with Polymers for Biomedical Studies.
- 385 Soft Matter **2010**, 6 (6), 1081–1091. https://doi.org/10.1039/B913621E.
- 386 (2) Stephan, M. T.; Irvine, D. J. Enhancing Cell Therapies from the Outside in: Cell Surface
- Engineering Using Synthetic Nanomaterials. Nano Today 2011, 6 (3), 309–325.
- 388 https://doi.org/https://doi.org/10.1016/j.nantod.2011.04.001.
- 389 (3) M., S. M.; H., G. J. Exploring and Engineering the Cell Surface Interface. *Science* (80-.).
- 390 **2005**, *310* (5751), 1135–1138. https://doi.org/10.1126/science.1106587.
- 391 (4) Dzamukova, M. R.; Naumenko, E. A.; Rozhina, E. V; Trifonov, A. A.; Fakhrullin, R. F.
- 392 Cell Surface Engineering with Polyelectrolyte-Stabilized Magnetic Nanoparticles: A Facile
- 393 Approach for Fabrication of Artificial Multicellular Tissue-Mimicking Clusters. *Nano Res.*
- **2015**, 8 (8), 2515–2532. https://doi.org/10.1007/s12274-015-0759-1.
- 395 (5) Stephan, M. T.; Moon, J. J.; Um, S. H.; Bershteyn, A.; Irvine, D. J. Therapeutic Cell
- Engineering with Surface-Conjugated Synthetic Nanoparticles. Nat. Med. 2010, 16 (9),

- 397 1035–1041. https://doi.org/10.1038/nm.2198.
- 398 (6) Sarkar, D.; Vemula, P. K.; Teo, G. S. L.; Spelke, D.; Karnik, R.; Wee, L. Y.; Karp, J. M.
- 399 Chemical Engineering of Mesenchymal Stem Cells to Induce a Cell Rolling Response.
- 400 Bioconjug. Chem. **2008**, 19 (11), 2105–2109. https://doi.org/10.1021/bc800345q.
- 401 (7) Lee, K.; Lee, J.; Jeong, E. J.; Kronk, A.; Elenitoba-Johnson, K. S. J.; Lim, M. S.; Kim, J.
- 402 Conjugated Polyelectrolyte-Antibody Hybrid Materials for Highly Fluorescent Live Cell-
- 403 Imaging. Adv. Mater. **2012**, 24 (18), 2479–2484. https://doi.org/10.1002/adma.201103895.
- 404 (8) Bailey, R. C.; Kwong, G. A.; Radu, C. G.; Witte, O. N.; Heath, J. R. DNA-Encoded
- 405 Antibody Libraries: A Unified Platform for Multiplexed Cell Sorting and Detection of
- 406 Genes and Proteins. J. Am. Chem. Soc. 2007, 129 (7), 1959–1967.
- 407 https://doi.org/10.1021/ja065930i.
- 408 (9) Li, W.; Bing, W.; Huang, S.; Ren, J.; Qu, X. Mussel Byssus-Like Reversible Metal-Chelated
- Supramolecular Complex Used for Dynamic Cellular Surface Engineering and Imaging.
- 410 Adv. Funct. Mater. **2015**, 25 (24), 3775–3784.
- 411 https://doi.org/https://doi.org/10.1002/adfm.201500039.
- 412 (10) Song, P.; Ye, D.; Zuo, X.; Li, J.; Wang, J.; Liu, H.; Hwang, M. T.; Chao, J.; Su, S.; Wang,
- 413 L.; Shi, J.; Wang, L.; Huang, W.; Lal, R.; Fan, C. DNA Hydrogel with Aptamer-Toehold-
- Based Recognition, Cloaking, and Decloaking of Circulating Tumor Cells for Live Cell
- 415 Analysis. *Nano Lett.* **2017**, *17* (9), 5193–5198.
- 416 https://doi.org/10.1021/acs.nanolett.7b01006.
- 417 (11) Carvajal-Hausdorf, D. E.; Schalper, K. A.; Neumeister, V. M.; Rimm, D. L. Quantitative

- Measurement of Cancer Tissue Biomarkers in the Lab and in the Clinic. *Lab. Investig.* **2015**,
- 419 95 (4), 385–396. https://doi.org/10.1038/labinvest.2014.157.
- 420 (12) You, M.; Lyu, Y.; Han, D.; Qiu, L.; Liu, Q.; Chen, T.; Sam Wu, C.; Peng, L.; Zhang, L.;
- Bao, G.; Tan, W. DNA Probes for Monitoring Dynamic and Transient Molecular
- Encounters on Live Cell Membranes. Nat. Nanotechnol. 2017, 12 (5), 453-459.
- 423 https://doi.org/10.1038/nnano.2017.23.
- 424 (13) Zhang, Y.; Üçüncü, M.; Gambardella, A.; Baibek, A.; Geng, J.; Zhang, S.; Clavadetscher,
- J.; Litzen, I.; Bradley, M.; Lilienkampf, A. Bioorthogonal Swarming: In Situ Generation of
- 426 Dendrimers. J. Am. Chem. Soc. 2020, 142 (52), 21615–21621.
- 427 https://doi.org/10.1021/jacs.0c07869.
- 428 (14) Thomsen, T.; Klok, H.-A. Chemical Cell Surface Modification and Analysis of
- Nanoparticle-Modified Living Cells. ACS Appl. Bio Mater. 2021, 4 (3), 2293–2306.
- 430 https://doi.org/10.1021/acsabm.0c01619.
- 431 (15) Nilsson, B.; Korsgren, O.; Lambris, J. D.; Ekdahl, K. N. Can Cells and Biomaterials in
- Therapeutic Medicine Be Shielded from Innate Immune Recognition? *Trends Immunol*.
- **2010**, *31* (1), 32–38. https://doi.org/http://dx.doi.org/10.1016/j.it.2009.09.005.
- 434 (16) Ramot, Y.; Steiner, M.; Morad, V.; Leibovitch, S.; Amouyal, N.; Cesta, M. F.; Nyska, A.
- Pulmonary Thrombosis in the Mouse Following Intravenous Administration of Quantum
- Dot-Labeled Mesenchymal Cells. *Nanotoxicology* **2010**, 4 (1), 98–105.
- 437 https://doi.org/10.3109/17435390903470093.
- 438 (17) Koo, H.; Choi, M.; Kim, E.; Hahn, S. K.; Weissleder, R.; Yun, S. H. Bioorthogonal Click

- 439 Chemistry-Based Synthetic Cell Glue. Small 2015, 11 (48), 6458–6466.
- 440 https://doi.org/https://doi.org/10.1002/sml1.201502972.
- 441 (18) Vogel, K.; Glettenberg, M.; Schroeder, H.; Niemeyer, C. M. DNA-Modification of
- 442 Eukaryotic Cells. *Small* **2013**, 9 (2), 255–262.
- 443 https://doi.org/https://doi.org/10.1002/smll.201201852.
- 444 (19) Tomás, R. M. F.; Gibson, M. I. Optimization and Stability of Cell-Polymer Hybrids
- Obtained by "Clicking" Synthetic Polymers to Metabolically Labeled Cell Surface Glycans.
- 446 *Biomacromolecules* **2019**, *20* (7), 2726–2736. https://doi.org/10.1021/acs.biomac.9b00478.
- 447 (20) Shi, P.; Ju, E.; Yan, Z.; Gao, N.; Wang, J.; Hou, J.; Zhang, Y.; Ren, J.; Qu, X.
- Spatiotemporal Control of Cell–Cell Reversible Interactions Using Molecular Engineering.
- Nat. Commun. 2016, 7 (1), 13088. https://doi.org/10.1038/ncomms13088.
- 450 (21) Medof, M. E.; Nagarajain, S.; Tykocinski, M. L. Cell-Surface Engineering with GPI-
- 451 Anchored Proteins. FASEB J. 1996, 10 (5), 574–586.
- 452 https://doi.org/https://doi.org/10.1096/fasebj.10.5.8621057.
- 453 (22) Wilson, J. T.; Krishnamurthy, V. R.; Cui, W.; Qu, Z.; Chaikof, E. L. Noncovalent Cell
- Surface Engineering with Cationic Graft Copolymers. J. Am. Chem. Soc. 2009, 131 (51),
- 455 18228–18229. https://doi.org/10.1021/ja908887v.
- 456 (23) Howarth, M.; Takao, K.; Hayashi, Y.; Ting, A. Y. Targeting Quantum Dots to Surface
- 457 Proteins in Living Cells with Biotin Ligase. *Proc. Natl. Acad. Sci. U. S. A.* **2005**, *102* (21),
- 458 7583 LP 7588. https://doi.org/10.1073/pnas.0503125102.
- 459 (24) Yao, C.; Tang, H.; Wu, W.; Tang, J.; Guo, W.; Luo, D.; Yang, D. Double Rolling Circle

- Amplification Generates Physically Cross-Linked DNA Network for Stem Cell Fishing. *J.*
- 461 Am. Chem. Soc. **2020**, 142 (7), 3422–3429. https://doi.org/10.1021/jacs.9b11001.
- 462 (25) Orynbayeva, Z.; Kolusheva, S.; Livneh, E.; Lichtenshtein, A.; Nathan, I.; Jelinek, R.
- Visualization of Membrane Processes in Living Cells by Surface-Attached Chromatic
- 464 Polymer Patches. *Angew. Chemie Int. Ed.* **2005**, 44 (7), 1092–1096.
- https://doi.org/https://doi.org/10.1002/anie.200462393.
- 466 (26) Chung, H. A.; Kato, K.; Itoh, C.; Ohhashi, S.; Nagamune, T. Casual Cell Surface
- 467 Remodeling Using Biocompatible Lipid-Poly(Ethylene Glycol)(n): Development of Stealth
- 468 Cells and Monitoring of Cell Membrane Behavior in Serum-Supplemented Conditions. J.
- 469 Biomed. Mater. Res. Part A **2004**, 70A (2), 179–185.
- 470 https://doi.org/https://doi.org/10.1002/jbm.a.20117.
- 471 (27) Weber, R. J.; Liang, S. I.; Selden, N. S.; Desai, T. A.; Gartner, Z. J. Efficient Targeting of
- Fatty-Acid Modified Oligonucleotides to Live Cell Membranes through Stepwise
- 473 Assembly. *Biomacromolecules* **2014**, *15* (12), 4621–4626.
- 474 https://doi.org/10.1021/bm501467h.
- 475 (28) Selden, N. S.; Todhunter, M. E.; Jee, N. Y.; Liu, J. S.; Broaders, K. E.; Gartner, Z. J.
- 476 Chemically Programmed Cell Adhesion with Membrane-Anchored Oligonucleotides. J.
- 477 Am. Chem. Soc. **2012**, 134 (2), 765–768. https://doi.org/10.1021/ja2080949.
- 478 (29) Baskin, J. M.; Prescher, J. A.; Laughlin, S. T.; Agard, N. J.; Chang, P. V; Miller, I. A.; Lo,
- 479 A.; Codelli, J. A.; Bertozzi, C. R. Copper-Free Click Chemistry for Dynamic in
- 480 Vivo Imaging. Proc. Natl. Acad. Sci. 2007, 104 (43), 16793 LP 16797.

- 481 https://doi.org/10.1073/pnas.0707090104.
- 482 (30) Swiston, A. J.; Cheng, C.; Um, S. H.; Irvine, D. J.; Cohen, R. E.; Rubner, M. F. Surface
- Functionalization of Living Cells with Multilayer Patches. *Nano Lett.* **2008**, 8 (12), 4446–
- 484 4453. https://doi.org/10.1021/nl802404h.
- 485 (31) Gendusa, R.; Scalia, C. R.; Buscone, S.; Cattoretti, G. Elution of High-Affinity (>10-9 KD)
- Antibodies from Tissue Sections: Clues to the Molecular Mechanism and Use in Sequential
- 487 Immunostaining. J. Histochem. Cytochem. **2014**, 62 (7), 519–531.
- 488 https://doi.org/10.1369/0022155414536732.
- 489 (32) Lan, H. Y.; Mu, W.; Nikolic-Paterson, D. J.; Atkins, R. C. A Novel, Simple, Reliable, and
- 490 Sensitive Method for Multiple Immunoenzyme Staining: Use of Microwave Oven
- Heating to Block Antibody Crossreactivity and Retrieve Antigens. *J. Histochem.*
- 492 *Cytochem.* **1995**, *43* (1), 97–102. https://doi.org/10.1177/43.1.7822770.
- 493 (33) Gabriele, G.; D., H. M.; Lucas, P. Multiplexed Protein Maps Link Subcellular Organization
- 494 to Cellular States. Science (80-.). **2018**, 361 (6401), eaar7042.
- 495 https://doi.org/10.1126/science.aar7042.
- 496 (34) Glass, G.; Papin, J. A.; Mandell, J. W. Simple: A Sequential Immunoperoxidase Labeling
- 497 and Erasing Method. J. Histochem. Cytochem. 2009, 57 (10), 899–905.
- 498 https://doi.org/10.1369/jhc.2009.953612.
- 499 (35) Zrazhevskiy, P.; Gao, X. Quantum Dot Imaging Platform for Single-Cell Molecular
- Profiling. *Nat. Commun.* **2013**, *4* (1), 1619. https://doi.org/10.1038/ncomms2635.
- 501 (36) Zrazhevskiy, P.; True, L. D.; Gao, X. Multicolor Multicycle Molecular Profiling with

- Quantum Dots for Single-Cell Analysis. Nat. Protoc. 2013, 8 (10), 1852–1869.
- 503 https://doi.org/10.1038/nprot.2013.112.
- 504 (37) Zhou, W.; Han, Y.; Beliveau, B. J.; Gao, X. Combining Qdot Nanotechnology and DNA
- Nanotechnology for Sensitive Single-Cell Imaging. Adv. Mater. 2020, 32 (30), 1908410.
- 506 https://doi.org/https://doi.org/10.1002/adma.201908410.
- 507 (38) Shi, P.; Zhao, N.; Coyne, J.; Wang, Y. DNA-Templated Synthesis of Biomimetic Cell Wall
- for Nanoencapsulation and Protection of Mammalian Cells. *Nat. Commun.* **2019**, *10* (1),
- 509 2223. https://doi.org/10.1038/s41467-019-10231-y.
- 510 (39) Shi, P.; Zhao, N.; Lai, J.; Coyne, J.; Gaddes, E. R.; Wang, Y. Polyvalent Display of
- Biomolecules on Live Cells. *Angew. Chemie Int. Ed.* **2018**, *57* (23), 6800–6804.
- 512 https://doi.org/10.1002/anie.201712596.
- 513 (40) Russ, J. C.; Neal, F. B. The Image Processing Handbook, 7th ed.; CRC Press, Inc.: USA,
- 514 2015.
- 515 (41) Deng, Y.; Shavandi, A.; Okoro, O. V.; Nie, L. Alginate Modification via Click Chemistry
- for Biomedical Applications. Carbohydr. Polym. 2021, 270, 118360.
- 517 https://doi.org/https://doi.org/10.1016/j.carbpol.2021.118360.
- 518 (42) Dirks, R. M.; Pierce, N. A. Triggered Amplification by Hybridization Chain Reaction. *Proc.*
- 519 Natl. Acad. Sci. U. S. A. **2004**, 101 (43), 15275–15278.
- 520 https://doi.org/10.1073/pnas.0407024101.
- 521 (43) Lim, K. S.; Lee, D. Y.; Valencia, G. M.; Won, Y.-W.; Bull, D. A. Cell Surface-Engineering
- to Embed Targeting Ligands or Tracking Agents on the Cell Membrane. *Biochem. Biophys.*

- 523 Res. Commun. **2017**, 482 (4), 1042–1047.
- 524 https://doi.org/https://doi.org/10.1016/j.bbrc.2016.11.155.
- 525 (44) Ma, S.; Xu, Y.; Song, W. Functional Bionanomaterials for Cell Surface Engineering in
- 526 Cancer Immunotherapy. *APL Bioeng.* **2021**, 5 (2), 21506.
- 527 https://doi.org/10.1063/5.0045945.
- 528 (45) Ko, I. K.; Kean, T. J.; Dennis, J. E. Targeting Mesenchymal Stem Cells to Activated
- 529 Endothelial Cells. *Biomaterials* **2009**, *30* (22), 3702–3710.
- https://doi.org/https://doi.org/10.1016/j.biomaterials.2009.03.038.
- 531 (46) Petersburg, J. R.; Shen, J.; Csizmar, C. M.; Murphy, K. A.; Spanier, J.; Gabrielse, K.;
- Griffith, T. S.; Fife, B.; Wagner, C. R. Eradication of Established Tumors by Chemically
- Self-Assembled Nanoring Labeled T Cells. ACS Nano 2018, 12 (7), 6563–6576.
- 534 https://doi.org/10.1021/acsnano.8b01308.
- 535 (47) Almeida, M.; García-Montero, A. C.; Orfao, A. Cell Purification: A New Challenge for
- Biobanks. *Pathobiology* **2014**, *81* (5–6), 261–275. https://doi.org/10.1159/000358306.
- 537 (48) Gerdes, M. J.; Sevinsky, C. J.; Sood, A.; Adak, S.; Bello, M. O.; Bordwell, A.; Can, A.;
- Corwin, A.; Dinn, S.; Filkins, R. J.; Hollman, D.; Kamath, V.; Kaanumalle, S.; Kenny, K.;
- Larsen, M.; Lazare, M.; Li, Q.; Lowes, C.; McCulloch, C. C.; McDonough, E.; Montalto,
- M. C.; Pang, Z.; Rittscher, J.; Santamaria-Pang, A.; Sarachan, B. D.; Seel, M. L.; Seppo,
- A.; Shaikh, K.; Sui, Y.; Zhang, J.; Ginty, F. Highly Multiplexed Single-Cell Analysis of
- Formalin-Fixed, Paraffin-Embedded Cancer Tissue. *Proc. Natl. Acad. Sci.* **2013**, 110 (29),
- 543 11982 LP 11987. https://doi.org/10.1073/pnas.1300136110.

- 544 (49) Drachuk, I.; Gupta, M. K.; Tsukruk, V. V. Biomimetic Coatings to Control Cellular
- Function through Cell Surface Engineering. Adv. Funct. Mater. 2013, 23 (36), 4437–4453.
- 546 https://doi.org/https://doi.org/10.1002/adfm.201300038.
- 547 (50) Orive, G.; Santos, E.; Poncelet, D.; Hernández, R. M.; Pedraz, J. L.; Wahlberg, L. U.; De
- Vos, P.; Emerich, D. Cell Encapsulation: Technical and Clinical Advances. Trends
- 549 *Pharmacol.* Sci. **2015**, 36 (8), 537–546.
- 550 https://doi.org/https://doi.org/10.1016/j.tips.2015.05.003.
- 551 (51) Calafiore, R.; Basta, G. Clinical Application of Microencapsulated Islets: Actual
- Prospectives on Progress and Challenges. Adv. Drug Deliv. Rev. 2014, 67–68, 84–92.
- 553 https://doi.org/https://doi.org/10.1016/j.addr.2013.09.020.
- 554 (52) Colton, C. K. Oxygen Supply to Encapsulated Therapeutic Cells. Adv. Drug Deliv. Rev.
- **2014**, 67–68, 93–110. https://doi.org/https://doi.org/10.1016/j.addr.2014.02.007.
- 556 (53) Wetmur, J. G.; Davidson, N. Kinetics of Renaturation of DNA. J. Mol. Biol. 1968, 31 (3),
- 557 349–370. https://doi.org/https://doi.org/10.1016/0022-2836(68)90414-2.
- 558 (54) Lee, C. S.; Davis, R. W.; Davidson, N. A Physical Study by Electron Microscopy of the
- Terminally Repetitious, Circularly Permuted DNA from the Coliphage Particles of
- 560 Escherichia Coli 15. *J. Mol. Biol.* **1970**, 48 (1), 1–22.
- 561 https://doi.org/https://doi.org/10.1016/0022-2836(70)90215-9.
- 562 (55) Meselson, M. S.; Radding, C. M. A General Model for Genetic Recombination. *Proc. Natl.*
- 563 Acad. Sci. 1975, 72 (1), 358 LP 361. https://doi.org/10.1073/pnas.72.1.358.
- 564 (56) Göpferich, A. Mechanisms of Polymer Degradation and Erosion. *Biomaterials* 1996, 17 (2),

565		103-114. https://doi.org/https://doi.org/10.1016/0142-9612(96)85755-3.
566	(57)	T., A.; W., M. E.; I., S. S. Functional Supramolecular Polymers. Science (80). 2012, 335
567		(6070), 813–817. https://doi.org/10.1126/science.1205962.
568		

569 For Table of Contents Only

